

Overcoming the Convex Relaxation Barrier for Neural Network Verification via Nonconvex Low-Rank Semidefinite Relaxations

Hong-Ming Chiu
University of Illinois at Urbana–Champaign
hmchiu2@illinois.edu

Richard Y. Zhang
University of Illinois at Urbana–Champaign
ryz@illinois.edu

December 1, 2022

Abstract

To rigorously certify the robustness of neural networks to adversarial perturbations, most state-of-the-art techniques rely on a triangle-shaped linear programming (LP) relaxation of the ReLU activation. While the LP relaxation is exact for a single neuron, recent results suggest that it faces an inherent “convex relaxation barrier” as additional activations are added, and as the attack budget is increased. In this paper, we propose a nonconvex relaxation for the ReLU relaxation, based on a low-rank restriction of a semidefinite programming (SDP) relaxation. We show that the nonconvex relaxation has a similar complexity to the LP relaxation, but enjoys improved tightness that is comparable to the much more expensive SDP relaxation. Despite nonconvexity, we prove that the verification problem satisfies constraint qualification, and therefore a Riemannian staircase approach is guaranteed to compute a near-globally optimal solution in polynomial time. Our experiments provide evidence that our nonconvex relaxation almost completely overcome the “convex relaxation barrier” faced by the LP relaxation.

1 Introduction

It is now well-known that neural network models can be vulnerable to adversarial perturbations, which are small, often imperceptible changes to the input that cause large, possibly targeted changes to the output [23, 1]. To make models robust to adversarial perturbation attacks, one popular strategy, known as *adversarial training* [12, 10, 13, 21, 29], is to attack a pre-trained model, and then to re-train the model with the training set augmented or replaced by the attack. Despite its simplicity, adversarial training works remarkably well in practice. For example, the robust models trained by Madry et al. [13] back in 2017 remain essentially unbroken in 2022, after more than four years of white-box penetration testing by researchers world-wide. Later researchers have extended the idea to train robust ImageNet classifiers, that achieve a similar level of accuracy, and within a comparable amount of training time, to nonrobust classifiers [21, 29]. Unfortunately, adversarial training is, in the end, an empirical strategy, that does not rigorously promise a truly robust model. Its use leaves open the possibility—however remote and unlikely—that a model that was previously thought to be robust would later be defeated by a more sophisticated attack, potentially after it has already been deployed out in the field.

For applications where even a single failure is deemed unacceptable, one often desires a formal mathematical proof or *certification* that an empirically robust model is truly robust against all future attacks. Most certification methods are based on a classical technique from optimization known as *convex relaxation*. The idea is to take the nonconvex set of viable attacks, and relax it into a larger, convex set of attacks, some (or almost all) of which may not be physically realizable. Irrespective of physical realizability, one can “efficiently” verify—i.e. in polynomial time—whether the model is truly robust against the entire convex superset of attacks. If this is indeed the case, then it immediately follows that the model is certifiably robust against all viable attacks, since these constitute a subset of the convex superset of attacks. However, if the model is not robust against the convex superset, then we must decline to make a certification. It may be the case that the model is not robust due to the existence of a viable attack. Or, the model may in fact be robust, but there exists a fictitious, non-physically-realizable attack within the convex superset that prevents us from certifying this fact.

Most state-of-the-art certification techniques [24, 26, 27, 30] are based on a triangle-shaped linear programming (LP) relaxation of the ReLU activation introduced by Wong and Kolter [28]. While the LP relaxation is *exact* for a single ReLU activation (i.e. it makes a certification if and only if there exists a viable attack), it quickly becomes loose as more activations are added, and as the attack budget is increased. Recent results by Salman et al. [20] indicate the existence of “convex relaxation barrier” for the LP relaxation. Every certification technique based on the LP relaxation is inherently limited to being a factor of 1.5 to 2 times more conservative for shallow model with 1-2 layers, and up to 10 times more conservative for a deeper model with 9 layers.

One promising pathway for overcoming the convex relaxation barrier faced by the LP relaxation is the semidefinite programming (SDP) relaxation of Raghunathan et al. [17]. Empirically, the SDP relaxation appears to be much *tighter* than the LP relaxation, in that it is able exclude far more fictitious attacks that cannot be physically realized. However, the cost of solving the SDP relaxation—while technically still polynomial time—is so large as to be completely inaccessible, even for tiny models with just a few hundred activations. At its core, the SDP relaxation requires us to optimize over the $\frac{1}{2}n(n+1)$ elements of an $n \times n$ symmetric matrix, where n is equal to the total number of ReLU activations, plus the dimension of the input layer. Even a single-layer model with 200 ReLU activations for the MNIST dataset would require us to optimize over the 4.84×10^5 elements of a 984×984 symmetric matrix, which is already nearing the limit of state-of-the-art solvers like MOSEK [14].

Contributions This paper proposes a certification technique based on a *nonconvex* relaxation for the ReLU activation. We argue that the set of viable attacks is naturally nonconvex, and as such a nonconvex relaxation should better exclude fictitious attacks when compared to a convex relaxation of a similar dimension or complexity. We base our nonconvex relaxation on a *low-rank restriction* of the usual convex SDP relaxation of the ReLU activation. Rigorously, we show that the nonconvex relaxation is always at least as tight as the SDP relaxation, but that it optimizes over the nr elements of an $n \times r$ rectangular matrix, where n is the same as before in the SDP relaxation, and r is a relaxation rank parameter. If a small value of r can be used (in practice, our experiments suggest a value of $r \leq 10$), then the nonconvex relaxation enjoys the same tightness and effectiveness of the SDP relaxation, while optimizing over a dramatically smaller number of variables that is comparable to the LP relaxation.

The nonconvexity of the relaxation poses a potential issue. Here, we adopt an approach known as the Riemannian staircase [2, 3], which allows nonconvex low-rank SDPs that satisfy a condition known as linear independence constraint qualification (LICQ) to be solved to near-global optimality

in polynomial time. Unfortunately, LICQ is highly restrictive and also difficult to verify in practice. It is often taken as a strong assumption in the existing literature [18, 7, 19], but this reduces the Riemannian staircase from a provable algorithm to an empirical heuristic. In this paper, we rigorously show that the verification problem generically satisfies LICQ. It immediately follows that our nonconvex relaxation can generically be solved to near-global optimality in polynomial time.

Our experiments provide empirical confirmation of our theoretical claims. We re-examine the models originally used by Salman et al. [20] to demonstrate the existence of a “convex relaxation barrier” for the LP relaxation. Using a relaxation rank r of no more than 10, we re-certify these models using our nonconvex relaxation, in time comparable to that of the best-possible LP relaxation. Our results find that even a basic nonconvex relaxation offers a significant reduction in conservatism, from factors of 2 to 10 down to a factor of around 1.1. Augmenting the nonconvex relaxation by bound propagation (as is commonly done for the LP relaxation) allows us to almost fully close the gap towards exact certification.

2 Background and related work

Consider the task of classifying a data point $\hat{x} \in \mathbb{R}^p$ as belonging to the \hat{c} -th of q classes. The standard approach is to train a classifier model $f_\theta : \mathbb{R}^p \rightarrow \mathbb{R}^q$ with parameters θ so that the prediction vector $f_\theta(\hat{x})$ takes on its maximum value at the \hat{c} -th element, as in $f_\theta(\hat{x})[\hat{c}] > f_\theta(\hat{x})[c]$ for all incorrect labels $c \neq \hat{c}$. In this paper, we focus our attention on ℓ -layer feedforward ReLU-based neural network models, defined recursively

$$x_1 \equiv x, \quad f_\theta(x) \equiv W_\ell x_\ell + b_\ell, \quad x_{k+1} = \max\{0, W_k x_k + b_k\} \quad \text{for } k \in \{1, 2, \dots, \ell\} \quad (1)$$

with respect to the parameters $\theta = \{W_k, b_k\}_{k=1}^\ell$, which consist of the weights W_1, \dots, W_ℓ and the biases b_1, \dots, b_ℓ . Throughout the paper, we will use n_k to denote the number of neurons at the k -th layer, and $n = \sum_{k=1}^\ell n_k$ to denote the total number of neurons summed over the entire neural network. Note that our convention includes the neurons at the input layer, i.e. those taking on values in $x_1 \equiv x$, but excludes those at the output layer, i.e. those taking on values of $f_\theta(x) \equiv W_\ell x_\ell + b_\ell$.

To compute an adversarial example $x \approx \hat{x}$, the standard approach (and usually, the most effective approach) is to apply projected gradient descent (PGD) to the following *semi-targeted attack* problem, which was first introduced by Carlini and Wagner [6]:

$$\phi[c] = \min_{x \in \mathbb{R}^p} f_\theta(x)[\hat{c}] - f_\theta(x)[c] \quad \text{s.t.} \quad \|x - \hat{x}\|_p \leq \rho. \quad (2)$$

Here, the attack budget is controlled by the parameter ρ , which specifies the maximum radius of the adversarial perturbation as measured in the ℓ_p norm. The attack is said to be semi-targeted because it seeks to rank the target class c above the true class \hat{c} , without necessarily requiring the target class c to be the top-ranked class. Nevertheless, applying PGD to (2) frequently results in misclassification to the target class c . In fact, for a non-robust model, only a single PCG iteration is usually enough for targeted misclassification to occur; the resulting one-iteration attack is called the fast gradient sign method (FGSM) attack, due to Goodfellow et al. [10]. Empirically robust models can be obtained by adversarially training a model against either the FGSM attack (as in Goodfellow et al. [10] and later Wong et al. [29]) or the PGD attack (as in Madry et al. [13] and [21]).

In turn, robustness to adversarial perturbations can be certified by verifying that (2) achieves a positive global minimum $\phi[c] > 0$ for every incorrect class $c \neq \hat{c}$. To explain, recall that $\phi[c]$ denotes the maximum margin by which an attack can cause the model f_θ to rank the incorrect label $c \neq \hat{c}$

above the true label \hat{c} . Clearly, if there exists no attack capable of ranking any incorrect label $c \neq \hat{c}$ above the true label \hat{c} , then the model is robust. In turn, the numerical value of the minimum global minimum, written

$$\phi^* = \min_{c \neq \hat{c}} \phi[c] > 0, \quad (3)$$

is a *robustness margin* that measures how robust the model is to adversarial perturbations. The more positive is the robustness margin ϕ^* , the more the model is able to resist misclassification.

Unfortunately, it is NP-hard in general to compute the global minimum $\phi[c]$, and therefore also the robustness margin ϕ^* [26]. While strategies like mixed-integer linear programming (MILP) [24] and Satisfiability Modulo Theories (SMT) [11] exist to compute these values exactly, their worst-case run time must scale exponentially with the number of activations, unless P=NP. Instead, most certification methods rely on solving (2) subject to a relaxation of the ReLU activation function in (1). In particular, Wong and Kolter [28] suggested the following triangle-shaped LP relaxation for a single ReLU activation:

$$\begin{aligned} \beta = \max\{0, \alpha\}, \\ \underline{\alpha} \leq \alpha \leq \bar{\alpha} \end{aligned} \quad \implies \quad \begin{aligned} \beta \geq 0, \quad \beta \geq \alpha, \\ \beta \leq \frac{\max\{0, \bar{\alpha}\} - \max\{0, \underline{\alpha}\}}{\bar{\alpha} - \underline{\alpha}} (\alpha - \underline{\alpha}) + \max\{0, \underline{\alpha}\} \end{aligned}$$

Extending this relaxation to all ReLU activations across all layers of a model requires upper- and lower-bounds $\underline{\alpha}, \bar{\alpha}$ on each pre-activation variable α ; recursive bound propagation procedures have been proposed to compute these efficiently [27, 26, 30, 20]. Substituting into the semi-targeted attack problem (2) results in a lower-bound $\phi_{\text{lb}}[c] \leq \phi[c]$ for the incorrect class $c \neq \hat{c}$. In turn, taking the minimum lower-bound $\phi_{\text{lb}}^* = \min_{c \neq \hat{c}} \phi_{\text{lb}}[c]$ among all incorrect classes results in a lower-bound $\phi_{\text{lb}}^* \leq \phi^*$ on the robustness margin. If $\phi_{\text{lb}}^* > 0$, then the model is robust, and its robustness margin is at least ϕ_{lb}^* .

The LP relaxation described above is easily verified to be tight for a single activation, meaning that it provides a lower-bound $\phi_{\text{lb}}[c] = \phi[c]$ that holds with equality. However, for many single activations, the relaxation is usually loose, meaning that the lower-bound $\phi_{\text{lb}}[c] < \phi[c]$ is strict. Indeed, Salman et al. [20] pointed out that the lower-bound is loose by a sizable margin, and that this gap cannot be improved. They refer to the inherent looseness of the LP relaxation as the “convex relaxation barrier”.

One promising direction that can potentially overcome the “convex relaxation barrier” is the SDP relaxation of Raghunathan et al. [17]. The relaxation is based on the insight that the ReLU activation equation can be equivalently imposed as two linear inequalities and a single quadratic equality

$$\beta = \max\{0, \alpha\} \quad \iff \quad \beta \geq 0, \quad \beta \geq \alpha, \quad \beta(\beta - \alpha) = 0.$$

Following a standard approach of Shor [22], it follows that the ReLU activation equation over a single layer can be written as the following linear inequalities

$$x_2 = \max\{0, W_1 x_1 + b_1\} \quad \iff \quad \begin{aligned} x_0 = 1, \quad x_2 \geq 0, \quad x_2 \geq W_1 x_1 + b_1, \\ \text{diag}(X_{22}) = \text{diag}(W_1 X_{12} + b_1 x_2^T), \end{aligned} \quad (4)$$

imposed over the following rank-1 matrix variable

$$X = \left[\begin{array}{c|cc} x_0 & x_1^T & x_2^T \\ \hline x_1 & X_{11} & X_{12} \\ x_2 & X_{12}^T & X_{22} \end{array} \right] \succeq 0, \quad \text{rank}(X) = 1.$$

The nonconvexity of the ReLU activation is entirely captured within the constraint $\text{rank}(X) = 1$. Relaxing this constraint results a convex relaxation, commonly known simply as “the” SDP relaxation.

In their original experiments, Raghunathan et al. [17] found that the simple SDP relaxation described became loose once it is applied to deeper models containing many layers. This empirical observation was later rigorously justified by the geometric analysis of Zhang [31]. Instead, Raghunathan et al. [17] proposed a bound propagation procedure—directly analogous to the LP relaxation—that allows the SDP relaxation to be tightened for deeper networks.

3 Rank-constrained SDP relaxation and its dual

Our goal in this paper is to develop better lower-bounds on the following instance of (2):

$$\begin{aligned} \phi[c] = \min_{x=(x_1, \dots, x_\ell) \in \mathbb{R}^n} \quad & w_\ell^T x_\ell + w_0 \equiv [(\mathbf{e}_c - \mathbf{e}_{\hat{c}})^T W_\ell] x_\ell + [(\mathbf{e}_c - \mathbf{e}_{\hat{c}})^T b_\ell] \\ \text{s.t.} \quad & x_{k+1} = \max\{0, W_k x_k + b_k\} \quad \text{for } k \in \{1, \dots, \ell - 1\} \\ & \|x_1 - \hat{x}\| \leq \rho. \end{aligned} \tag{A}$$

Here, we recall that to lower-bound the robustness margin $\phi_{\text{lb}}^* \leq \phi^*$, it suffices to lower-bound the semi-targeted problem $\phi_{\text{lb}}[c] \leq \phi[c]$ for every incorrect class $c \neq \hat{c}$, and then take the minimum $\phi_{\text{lb}}^* = \min_{c \neq \hat{c}} \phi_{\text{lb}}[c]$ among all incorrect classes.

Following existing work on the SDP relaxation, we begin by substituting the rank-1 SDP reformulation of the ReLU activation in (4) to the semi-targeted attack problem (A). But instead of deleting the rank-1 constraint altogether, we propose to slightly relax it to a rank- r constraint, where $r \geq 1$ is a *relaxation rank* parameter, to result in a family of *nonconvex* relaxations

$$\begin{aligned} \phi_r[c] = \min_{X \in \mathbb{S}^{n+1}} \quad & w_\ell^T x_\ell + w_0 x_0 \\ \text{s.t.} \quad & \text{tr}(X_1) - 2x_1^T \hat{x}_1 + x_0 \|\hat{x}_1\|^2 \leq x_0 \rho^2, \quad x_0 = 1 \quad (y_0, z_0) \\ & x_{k+1} \geq 0, \quad x_{k+1} \geq W_k x_k + b_k x_0, \quad (y_{k,1}, y_{k,2}) \\ & \text{diag}(X_{k+1} - W_k X_{k,(k+1)} - b_k x_{k+1}^T) = 0, \quad (z_k) \\ & \text{for all } k \in \{1, 2, \dots, \ell - 1\} \end{aligned} \tag{SDP- r }$$

whose optimization variable X is an $(n+1) \times (n+1)$ rank-constrained positive semidefinite matrix with bounded trace

$$X = \left[\begin{array}{c|ccc} x_0 & x_1^T & \cdots & x_\ell^T \\ \hline x_1 & X_{1,1} & \cdots & X_{1,\ell} \\ \vdots & \vdots & \ddots & \vdots \\ x_\ell & X_{1,\ell}^T & \cdots & X_{\ell,\ell} \end{array} \right] \succeq 0, \quad \text{rank}(X) \leq r, \quad \text{tr}(X) \leq R^2,$$

and we will assume throughout the paper that the trace bound R has been chosen large enough so that $\text{tr}(X^*) < R^2$ holds at optimality with a *strict inequality*. It follows from (4) that $r = 1$ instance of (SDP- r) coincides with (A) exactly. Due to our use of a rank upper-bound, every subsequent instance then provides a lower-bound on its previous relaxation:

$$\phi[c] = \phi_1[c] \geq \phi_2[c] \geq \cdots \geq \phi_{n+1}[c].$$

Finally, setting $r = n + 1$ has the same effect as deleting the rank constraint, because every $(n + 1) \times (n + 1)$ matrix can have rank at most $n + 1$. Therefore, the $r = n + 1$ instance coincides with the convex semidefinite relaxation as originally proposed by [16].

For relaxation ranks of $r < n + 1$, the corresponding nonconvex instances of (SDP- r) are NP-hard in general to solve to global optimality. Even if we are provided with a globally optimal solution X^* , there is generally no way to (rigorously) tell that X^* is indeed globally optimal. Instead, the most we can say is that X^* provides an upper-bound $w_\ell^T x_\ell^* + w_0 \geq \phi_r[c]$ on the optimal value of (SDP- r), which is itself intended to be a lower-bound $\phi_r[c] \leq \phi[c]$ on our original problem of interest (A). Of course, one cannot draw a definitive conclusion in either direction from an upper-bound on a lower-bound.

Instead, we seek to construct a lower-bound on the optimal value $\phi_r[c]$ of the relaxation (SDP- r), which would in turn lower-bound the optimal value $\phi[c]$ of the original problem (A). Our motivating insight is that all instances of (SDP- r), including those nonconvex instances for $r < n + 1$, have the *same* convex Lagrangian dual. Define dual variables $y = (y_0, \{y_{k,1}, y_{k,2}\}_{k=1}^\ell)$ and $z = (y_0, \{z_k\}_{k=1}^\ell)$ to correspond to the linear constraints in (SDP- r) as shown in parentheses. Then, the dual problem is written:

$$\max_{\substack{y \geq 0, z, \\ \mu \leq 0}} z_0 + R^2 \mu \text{ s.t. } S(y, z) \equiv \frac{1}{2} \left[\begin{array}{c|ccc} s_0 & s_1^T & s_2^T & \cdots & s_\ell^T \\ s_1 & S_{1,1} & S_{1,2} & & \\ s_2 & S_{1,2}^T & S_{2,2} & \ddots & \\ \vdots & & \ddots & \ddots & S_{(\ell-1),\ell} \\ s_\ell & & & S_{(\ell-1),\ell}^T & S_{\ell,\ell} \end{array} \right] \succeq \mu I, \quad (\text{SDD})$$

in which the components of the slack matrix are written

$$\begin{aligned} s_0 &= 2 \left[w_0 + y_0(\|\hat{x}\|^2 - \rho^2) + \sum_{k=1}^{\ell-1} b_k^T y_{k,2} - z_0 \right], \\ s_1 &= W_1^T y_{1,2} - 2\hat{x}y_0, \quad s_\ell = w_\ell - [Z_{(\ell-1)}b_{(\ell-1)} + y_{(\ell-1),1} + y_{(\ell-1),2}], \\ s_{k+1} &= W_{k+1}^T y_{(k+1),2} - (Z_k b_k + y_{k,1} + y_{k,2}) \quad \text{for } k \in \{1, \dots, \ell - 2\}, \\ S_{1,1} &= 2y_0 I, \quad S_{k,(k+1)} = -W_k^T Z_k, \quad S_{(k+1),(k+1)} = 2Z_k \quad \text{for } k \in \{1, \dots, \ell - 1\}, \end{aligned}$$

where $Z_k = \text{diag}(z_k)$ for all k . We therefore obtain the following lower-bound on semi-targeted attack problem in (A), which is valid for *any* choice of multipliers $y \geq 0$ and z .

Proposition 1 (Dual lower-bound). *Let X^* denote the global solution of (SDP- r) with rank $r \geq 1$. Then, any dual multipliers $y = (y_0, \{y_{k,1}, y_{k,2}\}_{k=1}^{\ell-1})$ and $z = (z_0, \{z_k\}_{k=1}^{\ell-1})$ that satisfy $y \geq 0$ provide the following lower-bound*

$$\phi[c] \geq \phi_r[c] \geq z_0 + R^2 \cdot \min\{0, \lambda_{\min}[S(y, z)]\}.$$

Let X^* denote the globally optimal solution for the convex instance of (SDP- r) with $r = n + 1$. It turns out that *strong duality* is satisfied in the convex case, meaning that there exists optimal multipliers y^*, z^* that exactly satisfy $\phi_{n+1}[c] = z_0^* + R^2 \cdot \min\{0, \lambda_{\min}[S(y^*, z^*)]\}$ and therefore *certify* the global optimality X^* via Proposition 1. In fact, SDP solvers are guaranteed to compute a primal feasible X and dual multipliers y, z that certify X to be ϵ near-globally optimal in at most $O(\sqrt{n} \log(1/\epsilon))$ iterations. However, each iteration requires costs up to $O(n^6)$ time and $O(n^4)$ memory, and this limits the maximum number of neurons n that can be considered in practice to no more than a few hundred to a thousand.

Now, suppose that the convex solution X^* is in fact low-rank, as in $r^* = \text{rank}(X^*) \ll n$. The statement below says that the *nonconvex* instance of (SDP- r) with $r = r^*$ also admits optimal multipliers y^*, z^* that certify global optimality.

Theorem 2 (Existence of global optimality certificate). *Let $r^* = \text{rank}(X^*)$, where X^* denotes the maximum-rank solution to the convex instance of (SDP- r) with $r = n+1$. Then, there exists optimal multipliers $y^* = (y_0^*, \{y_{k,1}^*, y_{k,2}^*\}_{k=1}^{\ell-1})$ and $z^* = (z_0^*, \{z_k^*\}_{k=1}^{\ell-1})$ that satisfy $y^* \geq 0$ and the following*

$$\phi_{r^*}[c] = z_0^* + R^2 \cdot \min\{0, \lambda_{\min}[S(y^*, z^*)]\}.$$

Proof. The convex instance of (SDP- r) satisfies the dual Slater's condition: the primal is feasible with $x_0 = 1$, $x_1 = \hat{x}$, $x_{k+1} = \max\{0, W_k x_k + b_k\}$, and $X_{i,j} = x_i x_j^T$, and the dual is strictly feasible with $y = \mathbf{1}$ and $z = 0$ and $\mu \rightarrow -\infty$. Therefore, strong duality holds, and there exists y^*, z^* that satisfy $y^* \geq 0$ and $\phi_{n+1}[c] = z_0^* + R^2 \cdot \min\{0, \lambda_{\min}[S(y^*, z^*)]\}$. Now, we observe that X^* is also feasible for the nonconvex instance of (SDP- r) with $r = \text{rank}(X^*)$. This proves that $\phi_{r^*}[c] \leq \phi_{n+1}[c]$, and therefore $\phi_{r^*}[c] = \phi_{n+1}[c]$ because of every larger $r_+ = r + 1$ gives a relaxation of the previous value of r . \square

Therefore, a simple idea is to directly solve the nonconvex instance of (SDP- r) with $r = r^* \ll n$. In the following section, we use an approach of Burer and Monteiro [4] to directly optimize over the $O(nr) = O(n)$ underlying degrees of freedom contained within a rank- r matrix X . This approach also produces dual multipliers y, z that certify the *local optimality* of the computed X . Our main result is that, if X is indeed globally optimal, then the dual multipliers y, z that certify the local optimality of X must also certify its global optimality via Proposition 1.

4 Solution via Nonlinear Programming

In order to expose the underlying degrees of freedom in the rank- r matrix X , we reformulate problem (SDP- r) into a low-rank factorization form first proposed by Burer and Monteiro [4]:

$$\begin{aligned} \phi_r[c] &= \min_{u_0, u, V} u_0 \cdot (w_\ell^T u_\ell) && \text{(BM-}r\text{)} \\ \text{s.t.} \quad & \|u_1 - u_0 \hat{x}\|^2 + \|V_1\|^2 \leq u_0^2 \rho^2, \quad u_0^2 = 1 && (y_0, z_0) \\ & u_0 \cdot u_{k+1} \geq 0, \quad u_0 \cdot (u_{k+1} - W_k u_k - b_k u_0) \geq 0, && (y_{k,1}, y_{k,2}) \\ & \text{diag}[(u_{k+1} - W_k u_k - b_k u_0) u_{k+1}^T + (V_{k+1} - W_k V_k) V_{k+1}^T] = 0, && (z_k) \\ & 1 + \sum_{k=1}^{\ell-1} (\|u_k\|^2 + \|V_k\|^2) \leq R^2, && (\mu) \end{aligned}$$

for all $k \in \{1, \dots, \ell - 1\}$, and over optimization variables are $u_0 \in \mathbb{R}$ and $u = (u_1, \dots, u_\ell) \in \mathbb{R}^n$ and $V = (V_1, \dots, V_\ell) \in \mathbb{R}^{n \times (r-1)}$. Problem (BM- r) is obtained by substituting the following into (SDP- r)

$$X = \begin{bmatrix} x_0 & x_1^T & \cdots & x_\ell^T \\ x_1 & X_{11} & \cdots & X_{1,\ell} \\ \vdots & \vdots & \ddots & \vdots \\ x_\ell & X_{1,\ell}^T & \cdots & X_{\ell,\ell} \end{bmatrix} = \begin{bmatrix} u_0 & 0 \\ u_1 & V_1 \\ \vdots & \vdots \\ u_\ell & V_\ell \end{bmatrix} \begin{bmatrix} u_0 & 0 \\ u_1 & V_1 \\ \vdots & \vdots \\ u_\ell & V_\ell \end{bmatrix}^T = UU^T. \quad (5)$$

The equivalence between these two problems follows because every $(n+1) \times (n+1)$ matrix X of rank r can be factored as $X = LL^T$ into a low-rank Cholesky factor L that is both lower-triangular and of dimensions $(n+1) \times r$.

The advantage of the formulation (BM- r) is that it reduces the number of explicit variables from the $\frac{1}{2}n(n+1) \approx \frac{1}{2}n^2$ in the original matrix X to $nr+1 \approx nr$ in the factor matrix U , while also allowing the positive semidefinite constraint $X \succeq 0$ to be enforced for free. For moderate values of $r \ll n$, the resulting instance of (BM- r) contains just $O(n)$ variables and constraints.

We propose solving (BM- r) as an instance of the standard-form nonlinear program,

$$\min_{\|x\| \leq R} f(x) \quad \text{s.t.} \quad g(x) \leq 0, \quad h(x) = 0, \quad (\text{NLP})$$

using a high-performance general-purpose solver like `fmincon` or `knitro`. These are primal-dual solvers, and are designed to output a primal point $x = (u_0, u, \text{vec}(V))$ that is *first-order optimal*, and dual multipliers $y = (y_0, \{y_{k,1}, y_{k,2}\}_{k=1}^\ell)$ and $z = (z_0, \{z_k\}_{k=1}^\ell)$ that *certify* the first-order optimality of x . Below, the notion of first-order optimality is taken from Nocedal and Wright [15, Theorem 12.3], and the notion of certifiability follows from the proof of [15, Theorem 12.1].

Definition 3. The point x is said to be *first-order optimal* if it satisfies the constraints $g(x) \leq 0$ and $h(x) = 0$, and there exists no escape path $x(t)$ that begins at $x(0) = x$ and makes a first-order improvement to the objective while satisfying all constraints, as in

$$f(x(t)) \leq f(x) - \delta t, \quad g(x(t)) \leq 0, \quad h(x(t)) = 0, \quad \text{for all } t \in [0, \epsilon] \quad (6)$$

for sufficiently small but nonzero $\delta > 0$ and $\epsilon > 0$.

Definition 4. The point x is said to be *certifiably first-order optimal* if it satisfies the constraints $g(x) \leq 0$ and $h(x) = 0$, and there exist dual multipliers y and z that satisfy the Karush–Kuhn–Tucker (KKT) equations:

$$\nabla f(x) + \nabla g(x)y + \nabla h(x)z = 0, \quad y \odot g(x) = 0, \quad y \geq 0. \quad (7)$$

The dual multipliers y and z are said to *certify* x as being first-order optimal.

Our main idea is to simply take the dual multipliers y, z computed by the nonlinear programming solver, round them $y \leftarrow \max\{0, y\}$ as necessary to ensure that $y \geq 0$, and then to plug them back into Proposition 1. Unfortunately, it is also possible for a primal point x to be first-order optimal without being certifiably so, i.e. they may not exist dual multipliers y, z to certify the first-order optimality of x . As a simple example, consider $f(x) = x$, $g(x) = x^2$, and $h(x) = 0$. The global minimum $x = 0$ is obviously first-order optimal, but it is impossible to find a multiplier $y \geq 0$ that satisfies $\nabla f(x) + y \nabla g(x) = 1 + 2xy = 0$ at this point $x = 0$. In this case, a nonlinear programming solver may fail to produce a set of dual multipliers y, z altogether.

Instead, we give a mild constraint qualification that guarantees the existence of dual multipliers y, z specifically for problem (BM- r). Concretely, we prove that if all of the ReLU activation functions are differentiable at the point x , then the linear independence constraint qualification (LICQ) is satisfied, so the nonconvex relaxation (BM- r) is also smooth at x .

Lemma 5 (Nonzero preactivation). *Let $x = (u_0, u_1, \dots, u_\ell, \text{vec}(V_1), \dots, \text{vec}(V_\ell))$ satisfy:*

$$\mathbf{e}_i^T (W_k u_k + b_k u_0) \neq 0, \quad \mathbf{e}_i^T W_k V_k \neq 0 \quad \text{for all } k \in \{1, \dots, \ell - 1\}, \quad i \in \{1, \dots, n_k\}. \quad (\text{NPCQ})$$

Then, x is first-order optimal if and only if there exist dual multipliers y and z to certify x as being first-order optimal. Moreover, the choice of dual multipliers y, z is unique.

It then follows from the uniqueness of the dual multipliers that, if x is indeed globally optimal, then the dual multipliers y, z that certify the local optimality of X must also certify its global optimality via Proposition 1.

Theorem 6 (Zero duality gap). *Let $r \geq r^*$ where r^* is defined in Theorem 2. If x is globally optimal and satisfies (NPCQ), then the dual multipliers y and z that certify x to be first-order optimal must also certify x to be globally optimal, as in*

$$\phi_r[c] = u_0 \cdot (w_\ell^T u_\ell) = z_0 + R^2 \cdot \max\{0, \lambda_{\min}[S(y, z)]\}.$$

Therefore, if a first-order optimal point x satisfies nonzero preactivation but yields a large duality gap, then either r is too small, or x is not globally optimal (it is either a suboptimal local minimum or a saddle-point). In either case, we suggest lifting to a higher relaxation rank $r_+ = r + 1$. With this higher relaxation rank r_+ , any first-order optimal point x from before—including the true global minimum of the rank- r problem if $r < r^*$ —is guaranteed to become a saddle point. The statement below gives a direction to escape the saddle-point and make a decrement.

Theorem 7 (Escape lifted saddle point). *Let $x = (u_0, \{u_k, V_k\}_{k=1}^\ell)$ be certifiably first-order optimal for (BM- r) with dual multipliers (y, z) . If x satisfies (NPCQ) and $\|x\| < R$ and $\gamma = -\lambda_{\min}[S(y, z)] > 0$, then the eigenvector $\xi = (\xi_0, \xi_1, \xi_2, \dots, \xi_\ell)$ that satisfies $\xi^T S(y, z) \xi = -\gamma \|\xi\|^2$ implicitly defines an escape path $x_+(t) = (u_0, \{u_{k,+}(t), V_{k,+}(t)\}_{k=1}^\ell)$ with*

$$u_{k,+}(t) = u_k + O(t^2), \quad V_{k,+}(t) = [V_k, 0] + t \cdot [0, u_k \xi_0 / u_0 + \xi_k] + O(t^2)$$

that makes a second-order improvement to the objective while satisfying all constraints, as in

$$f(x_+(t)) = f(x) - t^2 \gamma, \quad g(x_+(t)) \leq 0, \quad h(x_+(t)) = 0 \text{ for all } t \in [0, \epsilon]$$

for sufficiently small but nonzero $\epsilon > 0$.

To escape the lifted saddle-point in practice, it suffices to move along the *straight* path $\tilde{x}_+(t) = (u_0, \{\tilde{u}_{k,+}(t), \tilde{V}_{k,+}(t)\}_{k=1}^\ell)$

$$\tilde{u}_{k,+}(t) = u_k, \quad \tilde{V}_{k,+}(t) = [V_k, 0] + t \cdot [0, u_k \xi_0 / u_0 + \xi_k],$$

then solve for feasibility $g(x) \leq 0$ and $h(x) = 0$. Concretely, after computing a first-order optimal x , we increment the relaxation rank $r_+ = r + 1$, and initialize the nonlinear programming solver using the lifted point $\tilde{x}_+(\epsilon)$ as the initial primal point, and the old multipliers y, z as the initial dual multipliers. If this arrives at the global optimum, then the corresponding y, z must certify x as being so. Otherwise, we repeat the rank lifting procedure.

Progressively lifting the relaxation rank r , in our experience it takes no more than $r \leq 10$ to reduce the duality gap to values of 10^{-8} . To rigorously guarantee a zero duality gap, however, can require a relaxation rank on the order of $r = O(\sqrt{n})$ [3], irrespective of the value of r^* . Indeed, counterexamples with $\epsilon_{\text{feas}} > 0$ exist for relaxation ranks r that are even slightly smaller than this threshold [25, 32]. As a purely theoretical result, the ability to achieve a zero duality gap implies that the nonconvex relaxation (with $r \geq r^*$) can be solved in polynomial time (and is therefore not NP-hard). Of course, setting $r = O(\sqrt{n})$ would also force us to optimize over $O(n^{3/2})$ variables, thereby offsetting much of our computational advantage against the usual convex SDP relaxation in practice.

Algorithm 1 summarizes our proposed approach in pseudocode form, and introduces a number of small practical refinements. The algorithm is, at its core, a special instance of the Riemannian staircase [2, 3], and as such bears similarities to related work in [18, 7, 8, 19]. However, our specialization to the verification setting enjoys much stronger guarantees, summarized in Theorem 6 and Theorem 7, because we are able to formally establish constraint qualification in Lemma 5. In contrast, prior work often take LICQ as a strong assumption, but this reduces the Riemannian staircase from a rigorous algorithm to an empirical heuristic.

Algorithm 1 Summary of proposed algorithm

Input: Initial relaxation rank $r \geq 2$. Weights W_1, \dots, W_ℓ and biases b_1, \dots, b_ℓ for the neural network. Original input \hat{x} , true label \hat{c} , target label c , and perturbation size ρ . Variable radius bound R .

Output: Lower-bound $\phi_{\text{lb}}[c] \leq \phi[c]$ on the optimal value of the semi-targeted attack problem (A).

Algorithm:

1. (Solve rank- r relaxation) Use a nonlinear programming solver to solve the following

$$\begin{aligned}
 \min_{\|x\| \leq R} \quad & f(x) \equiv (\mathbf{e}_c - \mathbf{e}_{\hat{c}})^T (W_\ell u_\ell u_0 + b_\ell) \\
 \text{s.t.} \quad & g_0(x) \equiv \|u_1 - u_0 \hat{x}\|^2 + \|V_1\|^2 - \rho^2 \leq 0 \quad (y_0) \\
 & h_0(x) \equiv 1 - u_0^2 = 0 \quad (z_0) \\
 & g_k(x) \equiv \begin{bmatrix} -u_0 u_{k+1} \\ u_0 (W_k u_k + b_k u_0 - u_{k+1}) \end{bmatrix} \leq 0 \quad (y_{k,1}, y_{k,2}) \\
 & h_k(x) \equiv \text{diag}[(u_{k+1} - W_k u_k - b_k u_0) u_{k+1}^T + (V_{k+1} - W_k V_k) V_{k+1}^T] = 0 \quad (z_k)
 \end{aligned}$$

for all $k \in \{1, 2, \dots, \ell - 1\}$ and over $x = (u_0, u_1, \dots, u_\ell, \text{vec}(V_1), \dots, \text{vec}(V_\ell))$. Retrieve the corresponding dual multipliers $y = (y_0, \{y_{k,1}, y_{k,2}\}_{k=1}^\ell)$ and $z = (z_0, \{z_k\}_{k=1}^\ell)$.

2. (Check certifiable first-order optimality) If $\|\nabla f(x) + \nabla g(x)y + \nabla h(x)z\|$ is sufficiently small, and if $g(x) \leq 0$ and $h(x) = 0$ and $\|x\| < R$ hold to sufficient tolerance, then continue. Otherwise, return error due to solver's inability to achieve certifiable first-order optimality.
3. (Check dual feasibility) If $\epsilon_{\text{feas}} = -\lambda_{\min}[S(y, z)]$ is sufficiently small, where the slack matrix $S(y, z)$ is defined in (SDD), then return $\phi_{\text{lb}}[c] = z_0 - \epsilon_{\text{feas}} \cdot R$. Otherwise, continue.
4. (Escape lifted saddle point) Compute the eigenvector $\xi = (\xi_0, \xi_1, \dots, \xi_\ell)$ satisfying $\|\xi\| = 1$ and $\xi^T S(y, z) \xi = -\epsilon_{\text{feas}}$. Set up new primal initial point $x_+ = (u_0, u_1, \dots, u_\ell, \text{vec}(V_{+,1}), \dots, \text{vec}(V_{+,\ell}))$ where

$$V_{+,k} = [V, 0] + \epsilon \cdot [0, u_k \xi_0 / u_0 + \xi_k].$$

Increment $r \leftarrow r + 1$ and repeat Step 1 with (x_+, y, z) as the initial point.

5 Experiments

In this section, we compare the practical performance of our proposed verifier **BM** to LP-based verifiers for certifying both ℓ_2 and ℓ_∞ adversaries. In addition, we also perform simulation on **BM-Full**, which is an extension of **BM** with the addition of pre-activation bounds on each hidden neuron. The detail formulation for **BM-Full** can be found in the Appendix.

Methods **BM** denotes the proposed method in the main paper. **BM-Full** denotes the proposed method with preactivation bounds. **PGD** denotes the projected gradient descent algorithm for finding the upper bound of (A). We compare **BM** and **BM-Full** to three LP-based verifiers: **LP-Full**, **CROWN-Ada** and **Fast-Lip**. **LP-Full** [20] is the optimal LP-relaxed verifier that uses the tightest possible pre-activation bounds by solving LP problems for each hidden neuron. **CROWN-Ada** [33] is a fast LP-relaxed verifier that uses the adaptive linear bounds on activations. **Fast-Lip** [26] is a fast robustness verifier based on propagating Lipschitz constant. Throughout out this experimental section, we set the preactivation bounds in **BM-Full** to be the same as those used in **LP-Full**.

Simulation environment. All simulations in this section are conducted on a computer with Apple silicon M1 pro chip with 10-core CPU, 16-core GPU, and 32GB of RAM. We implement **BM** and **BM-Full** in MATLAB, the non-convex relaxation problem (**BM- r**) is solved via trust-region interior-point solver KNITRO [5] with warm-start strategy. Due to the space constraints, we defer the detailed implementation for **BM** and **BM-Full** to the Appendix.

Model architectures We perform extensive simulation using three types of feed forward ReLU networks trained on MNIST dataset [9]: **NOR-MNIST**, **ADV-MNIST** and **LPD-MNIST**. All three models are fully connected neural networks that have 2 hidden layers with 100 neurons each. **NOR-MNIST** is normally trained using cross-entropy loss. **ADV-MNIST** is adversarially trained to against **PGD** attack using the method of [13], with ℓ_∞ radius equals to 0.1. **LPD-MNIST** is robustly trained via adversarial polytope perturbation by [28], with the size of the adversarial polytope being 0.1. All three models are adopted from [20]. Additionally, we use **MLP- $m \times n$** to denote a fully connected neural network of m hidden layers of n neurons each. All **MLP- $m \times n$** are adversarially trained using [13] with ℓ_∞ radius equals to 0.1.

5.1 Robustness verification on neural network inputs.

One important aspect of robust verification in image classification is to verify whether a correctly classified image is indeed robust at a radius ρ . Intuitively, most correct images of a robustly trained model should also be robust. To demonstrate the efficacy of our proposed method, in this experiment, we apply **BM** and **BM-Full** to verify robustness of correctly classified images for a robustly trained model.

In robust verification, we mark an image \hat{x} as *certified robust* within a norm ball of radius ρ if the lower bound on (A) is positive with respect to all 9 incorrect classes of \hat{x} , and mark an image \hat{x} as *not robust* if an attack is found by **PGD**; for **BM** and **BM-Full** the lower bound on (A) is given by Proposition 1. Additionally, for images that can neither be attacked by **PGD** nor certified by a verifier, we mark them as *status unknown*.

Results and discussions. Figure 1 shows the bar chart of the number of images that are *certified robust*, *status unknown* and *not robust* within the first 1000 images for **ADV-MNIST**. We compare the results form our **BM**-based verifier to LP-based verifiers, **LP-Full**, **CROWN-Ada** and **Fast-Lip**,

with respect to three different perturbation radius. In Figure 1, we show that our verifiers are able to consistently outperform all LP-based verifiers under different perturbation radii. Notably, for small perturbation, our verifiers can nearly certify all images that cannot be attacked by PGD, leaving a very small portion of images that are *status unknown*. This confirms the robust training method from [13] is indeed effective.

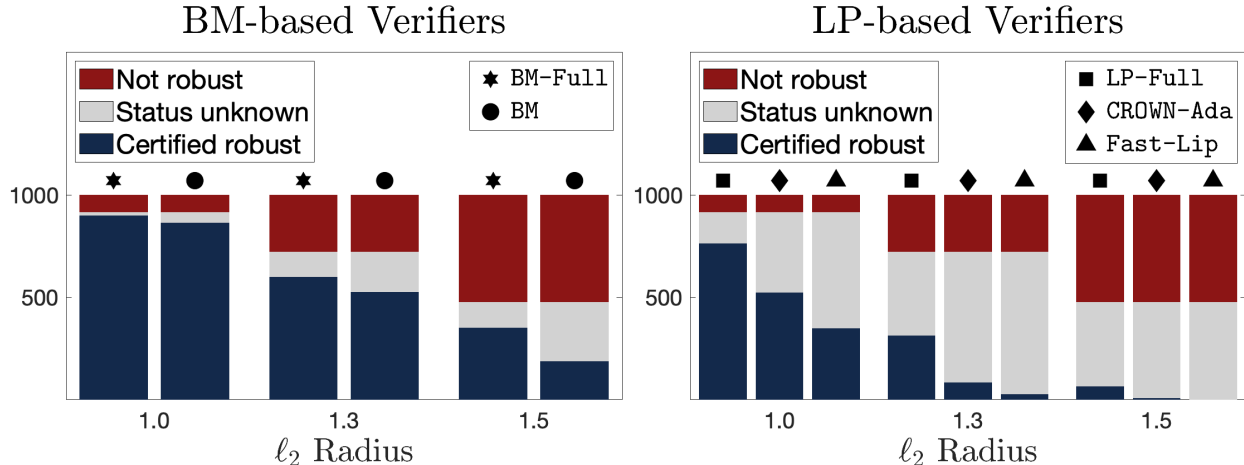


Figure 1: **Robustness verification for ADV-MNIST with ℓ_2 norm.** We compare the number of images verified within the first 1000 images for three different ℓ_2 perturbation radius, 1.0, 1.3 and 1.5. Each image has three possible status. (1) **Not robust (colored red)**: an attack has been found by PGD. (2) **Status unknown (colored gray)**: PGD cannot find an attack, but the verifier fail to certify robustness. (3) **Certified robust (colored blue)**: the verifier successfully certify robustness. We compare the verification results from our verifiers to those from others. (**Left.**) Our verifiers based on BM: BM-Full and BM. (**Right.**) Other verifiers based on LP: LP-Full, CROWN-Ada and Fast-Lip.

5.2 Tightness of our lower bound.

Since robust verification is an NP-hard problem, all relaxation methods must become loose for sufficiently large radius. Fortunately, robust verification is only need when the PGD upper bound of (A) is positive; therefore, we only need the relaxation to be tight when the PGD upper bound is still positive. In this experiment, we analyze the gap between our lower bound in Proposition 1 and the PGD upper bound over a wide range of perturbation radius.

To accurately measure the gap between our lower bound and the PGD upper bound, we average each bound over all 9 incorrect classes of the first 10 correctly classified images in the test set, in total 90 samples are considered.

Results and discussions. Figures 2 shows the average PGD upper bound, and the average lower bound on (A) computed from BM, BM-Full, LP-Full, CROWN-Ada and Fast-Lip for ADV-MNIST. As illustrated in Figure 2, our lower bounds are significantly tighter than all the other verifiers across a wide range of ℓ_2 and ℓ_∞ perturbation radius. Most importantly, our lower bounds are able to remain tightness in regions where the PGD upper bound is still positive.

The huge gap between LP-based verifiers and the PGD upper bound has been pointed out by [20], where he discover that even the optimal LP-relaxed verifier, the LP-Full in our experiment, is still subject to a theoretical limit: the convex relaxation barrier. Specifically, there exists an inherent

tradeoff between tightness and tractability, while LP-based verifiers are highly tractable, there is a fundamental limit on the level of tightness that the underlying relaxation problem could achieve. The results in Figure 2 show that our proposed method BM and BM-Full, which is based on solving nonconvex SDP relaxation via rank- r Burer-Monteiro, is able to overcome convex relaxation barrier and at the same time maintain computational tractable.

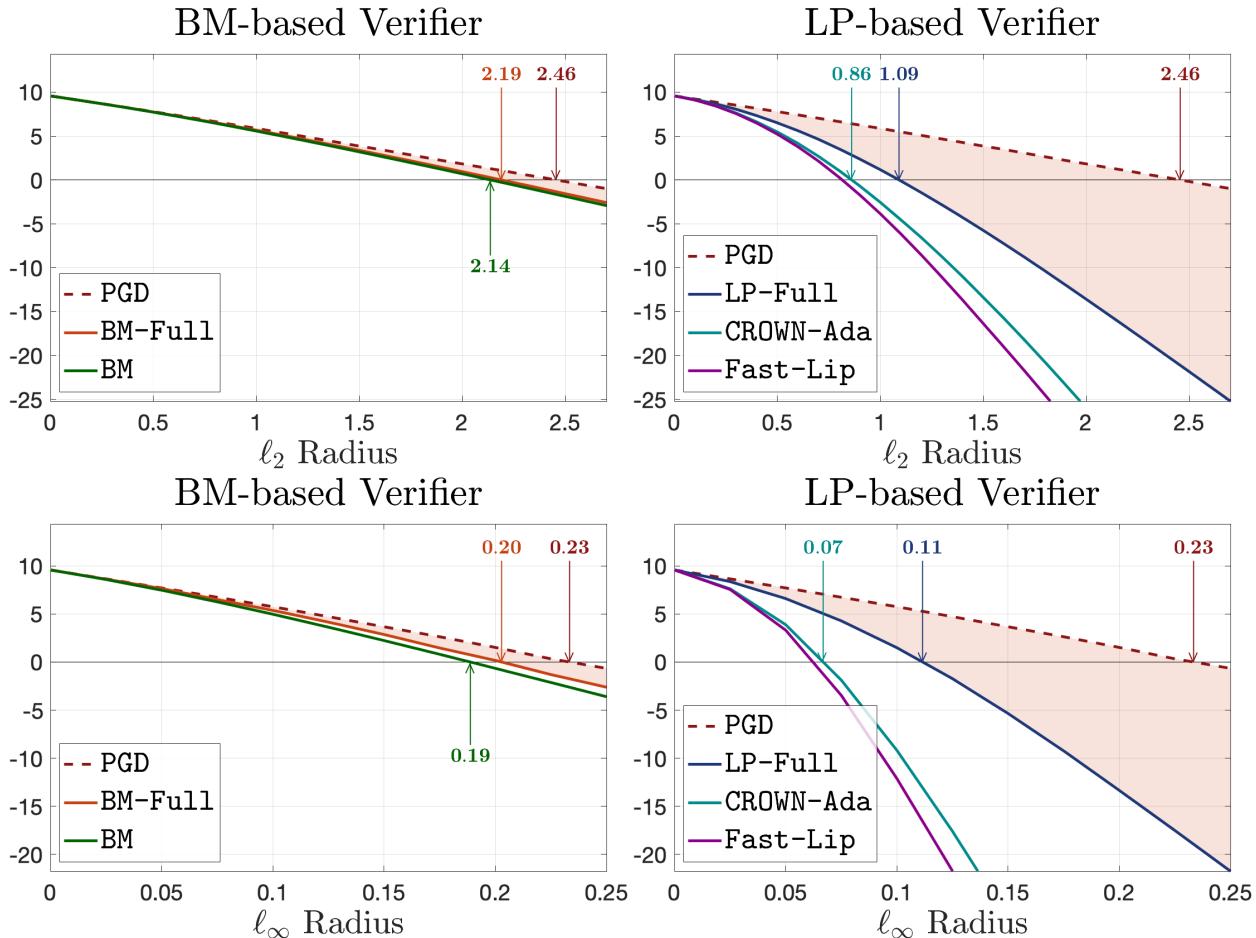


Figure 2: **Tightness of our lower bound on (A) for ADV-MNIST.** We compute the average lower bound on (A) using each verifier and compare it to the average PGD upper bound over a wide range of perturbation radius. The averages are taken over the first 10 images. **(Top row.)** ℓ_2 perturbation. **(Bottom row.)** ℓ_∞ perturbation. **(Left column.)** Our verifiers based on BM: BM-Full and BM. **(Right column.)** Other verifiers based on LP: LP-Full, CROWN-Ada and Fast-Lip.

5.3 Visualizing adversarial attacks and robustness verification

To illustrate why robustness verification is important in image classification, in this experiment, we perform a case study based on an image in the test set using the model ADV-MNIST. In particular, we focus on showing how would the ℓ_2 adversaries look like in practice for four perturbation radius $\rho \in \{0.5, 1.0, 1.7, 2.0\}$, as well as their corresponding lower bound on (A) computed from BM-based and LP-based verifiers. We choose ℓ_2 norm over ℓ_∞ norm for this experiment because ℓ_2 norm

allows perturbations to be concentrated on a small group of pixels, which produces adversaries that are more perceptually consistent to the original dataset when the perturbation radius is large.

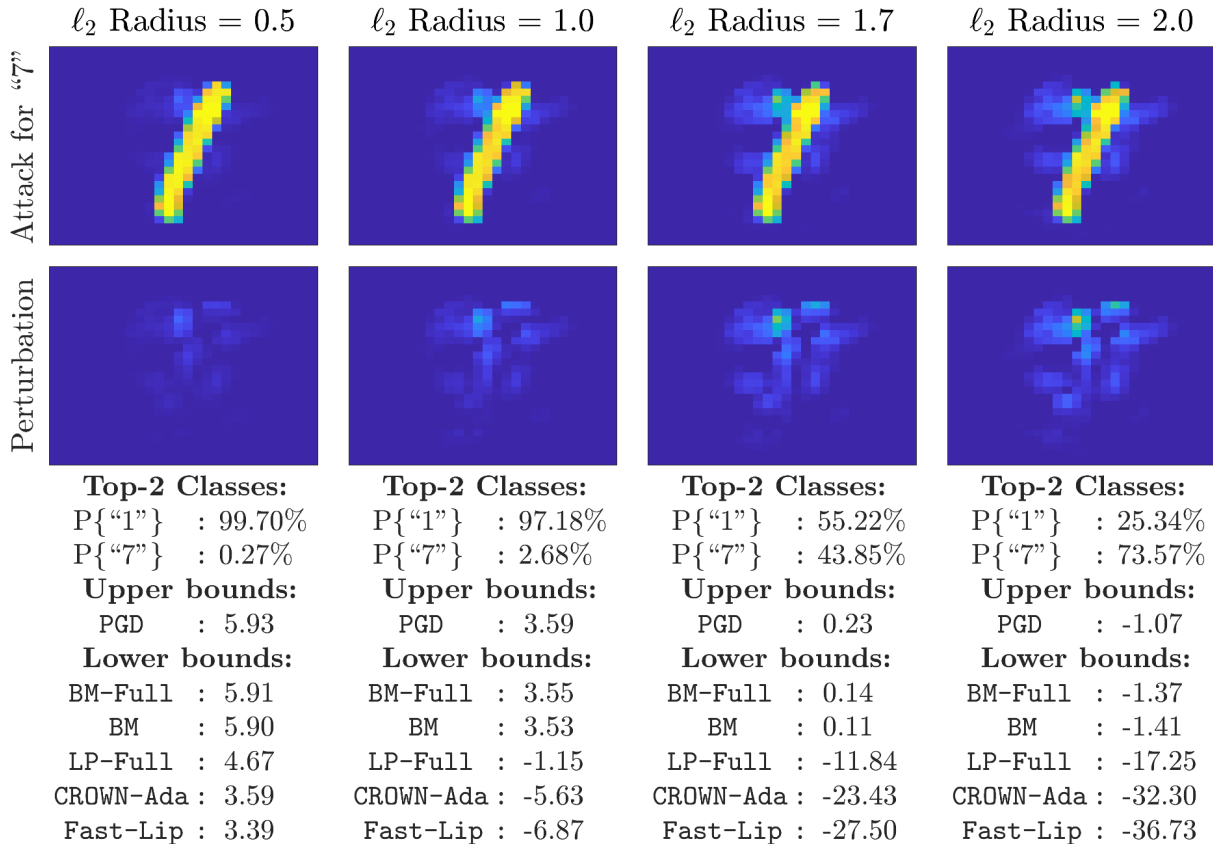


Figure 3: **Visualizing ℓ_2 adversarial examples for ADV-MNIST.** We take an image in the test set to compare the capability of different verifiers for certifying robustness within four different ℓ_2 radius $\rho \in \{0.5, 1.0, 1.7, 2.0\}$. Each column in the figure shows (left to right): **(Column 1.)** The image is robust for $\rho = 0.5$, and it can be certified by all verifiers. **(Column 2.)** The image is robust for $\rho = 1.0$, but it can be only be certified by our verifiers, BM-Full1 and BM. **(Column 3.)** The image is closed to become not robust for $\rho = 1.7$, but it can still be certified by our verifiers. **(Column 4.)** The image is not robust for $\rho = 2.0$.

Results and discussions. Figure 3 shows: the adversarial attacks targeting the second most probable class of a MNIST image of class "1"; the probability of the top-2 classes for the attacked image (calculated using the softmax function); the PGD upper bound; and the lower bounds from different verifiers. For the MNIST image shown in the figure, the second most probable class is "7", and its adversarial attacks are computed via PGD.

The first and second column of Figure 3 correspond to attacks within two small ℓ_2 perturbation radius $\rho \in \{0.5, 1.0\}$. We see that every verifiers is able to verify robustness for $\rho = 0.5$, however, only BM-Full1 and BM are able to verify robustness for $\rho = 1.0$, all the other verifiers fail because their corresponding lower bounds become loose. In both cases, the adversaries look really similar to the original image.

The third and fourth column of Figure 3 correspond to attack within two large ℓ_2 perturbation radius $\rho \in \{1.7, 2.0\}$. Notice that BM-Full1 and BM can still verify robustness for $\rho = 1.7$ even

though the image is at the boundary of becoming not robust. In addition, the image is not robust for $\rho = 2.0$ as the PGD upper bound is negative. Notably, both images start gaining features of the digit "7".

5.4 Tightness plots for deeper neural networks

It is known that the relaxation gap generally increases along with the number of layers in the neural network. To demonstrate the performance of our proposed methods in deeper networks, in this experiment, we measure the gap of BM-Full and BM with respect to models of three different depths.

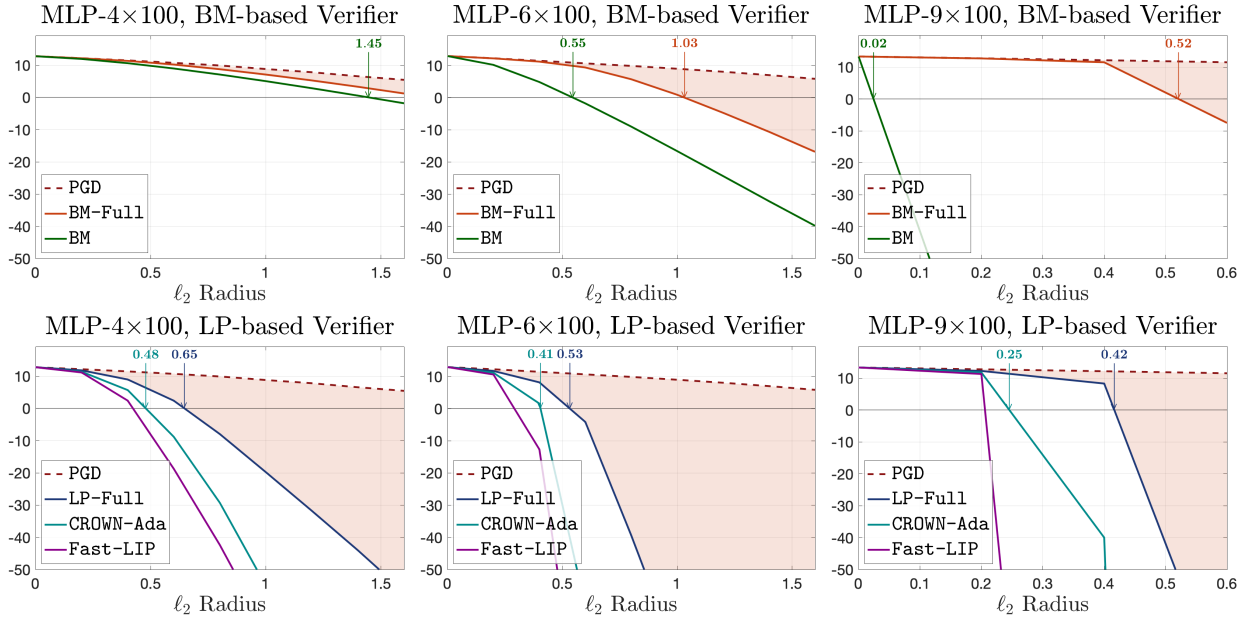


Figure 4: **Lower bound on (A) with different model depth (ℓ_2 norm).** We compute the average lower bound on (A) for three models with 4, 6, 9 hidden layers of 100 neuron each, respectively. The upper bound on robustness margin is estimated via PGD. Observe that the gap between the PGD upper bound and lower bound from BM-Full are significantly smaller than that from LP-Full. We note that without bound propagations, BM does get loose when the number of hidden layer is more than 6. (**Top row.**) Our verifiers, BM-Full and BM. (**Bottom row.**) Other verifiers: LP-Full, CROWN-Ada and Fast-Lip.

Results and discussions. Figure 4 plots the average bounds against ℓ_2 perturbation radius for three MLP networks with 4, 6, 9 hidden layers of 100 neurons each. Notably, BM become loose for MLP-6x100 and become looser than LP-Full for MLP-9x100. This result is expected and is consistent with [31]; in particular, the SDP relaxation for ReLU gate, without any bound constrains on preactivations, does become loose for multiple layers. On the other hand, BM-Full remain significantly tighter than LP-Full for all cases. Furthermore, since the preactivation bounds used in BM-Full and LP-Full are the same in this experiment, Figure 2 and Figure 4 suggest that with the same quality of preactivation bounds, BM-Full would yield a tighter relaxation than LP-Full. Based on this finding, we note that the preactivation bounds for BM-Full can also be computed via BM-based methods, which should yield a tighter bound on the preactivations and hence further

reduces the relaxation gap for **BM-Full**; one example would be recursively apply **BM-Full** to compute the upper and lower bound on each neuron, however, such method can be extremely computational expensive for small to medium size networks. We leave **BM-Full** with better preactivation bounds to our future work.

Acknowledgments

The authors thank Zico Kolter for insightful discussions and pointers to the literature. Financial support for this work was provided by the NSF CAREER Award ECCS-2047462 and C3.ai Inc. and the Microsoft Corporation via the C3.ai Digital Transformation Institute.

References

- [1] Battista Biggio, Iginio Corona, Davide Maiorca, Blaine Nelson, Nedim Srndic, Pavel Laskov, Giorgio Giacinto, and Fabio Roli. Evasion attacks against machine learning at test time. In *Joint European conference on machine learning and knowledge discovery in databases*, pages 387–402. Springer, 2013.
- [2] Nicolas Boumal, Vlad Voroninski, and Afonso Bandeira. The non-convex Burer-Monteiro approach works on smooth semidefinite programs. In *Advances in Neural Information Processing Systems*, pages 2757–2765, 2016.
- [3] Nicolas Boumal, Vladislav Voroninski, and Afonso S Bandeira. Deterministic guarantees for Burer-Monteiro factorizations of smooth semidefinite programs. *Communications on Pure and Applied Mathematics*, 73(3):581–608, 2020.
- [4] Samuel Burer and Renato DC Monteiro. A nonlinear programming algorithm for solving semidefinite programs via low-rank factorization. *Mathematical Programming*, 95(2):329–357, 2003.
- [5] Richard H Byrd, Jorge Nocedal, and Richard A Waltz. Knitro: An integrated package for nonlinear optimization. In *Large-scale nonlinear optimization*, pages 35–59. Springer, 2006.
- [6] Nicholas Carlini and David Wagner. Towards evaluating the robustness of neural networks. In *2017 IEEE Symposium on Security and Privacy (SP)*, pages 39–57. IEEE, 2017.
- [7] Luca Carlone, David M Rosen, Giuseppe Calafiore, John J Leonard, and Frank Dellaert. Lagrangian duality in 3d slam: Verification techniques and optimal solutions. In *2015 IEEE/RSJ International Conference on Intelligent Robots and Systems (IROS)*, pages 125–132. IEEE, 2015.
- [8] Jeremy Cohen, Elan Rosenfeld, and Zico Kolter. Certified adversarial robustness via randomized smoothing. In *International Conference on Machine Learning*, pages 1310–1320, 2019.
- [9] Li Deng. The mnist database of handwritten digit images for machine learning research. *IEEE Signal Processing Magazine*, 29(6):141–142, 2012.
- [10] Ian Goodfellow, Jonathon Shlens, and Christian Szegedy. Explaining and harnessing adversarial examples. In *International Conference on Learning Representations*, 2015. URL <http://arxiv.org/abs/1412.6572>.

- [11] Guy Katz, Clark Barrett, David L Dill, Kyle Julian, and Mykel J Kochenderfer. Reluplex: An efficient SMT solver for verifying deep neural networks. In *International Conference on Computer Aided Verification*, pages 97–117. Springer, 2017.
- [12] Alexey Kurakin, Ian Goodfellow, and Samy Bengio. Adversarial machine learning at scale. *arXiv preprint arXiv:1611.01236*, 2016.
- [13] Aleksander Madry, Aleksandar Makelov, Ludwig Schmidt, Dimitris Tsipras, and Adrian Vladu. Towards deep learning models resistant to adversarial attacks. In *International Conference on Learning Representations*, 2018.
- [14] ApS MOSEK. The MOSEK optimization toolbox for MATLAB manual, 2019. URL <https://docs.mosek.com/9.0/toolbox.pdf>.
- [15] Jorge Nocedal and Stephen Wright. *Numerical optimization*. Springer Science & Business Media, 2006.
- [16] Aditi Raghunathan, Jacob Steinhardt, and Percy Liang. Certified defenses against adversarial examples. In *International Conference on Learning Representations*, 2018.
- [17] Aditi Raghunathan, Jacob Steinhardt, and Percy S Liang. Semidefinite relaxations for certifying robustness to adversarial examples. In S. Bengio, H. Wallach, H. Larochelle, K. Grauman, N. Cesa-Bianchi, and R. Garnett, editors, *Advances in Neural Information Processing Systems 31*, pages 10900–10910. Curran Associates, Inc., 2018.
- [18] David M Rosen, Michael Kaess, and John J Leonard. Rise: An incremental trust-region method for robust online sparse least-squares estimation. *IEEE Transactions on Robotics*, 30(5):1091–1108, 2014.
- [19] David M Rosen, Luca Carlone, Afonso S Bandeira, and John J Leonard. Se-sync: A certifiably correct algorithm for synchronization over the special euclidean group. *The International Journal of Robotics Research*, 38(2-3):95–125, 2019.
- [20] Hadi Salman, Greg Yang, Huan Zhang, Cho-Jui Hsieh, and Pengchuan Zhang. A convex relaxation barrier to tight robustness verification of neural networks. *Advances in Neural Information Processing Systems*, 32, 2019.
- [21] Ali Shafahi, Mahyar Najibi, Mohammad Amin Ghiasi, Zheng Xu, John Dickerson, Christoph Studer, Larry S Davis, Gavin Taylor, and Tom Goldstein. Adversarial training for free! *Advances in Neural Information Processing Systems*, 32, 2019.
- [22] N.Z. Shor. Quadratic optimization problems. *Soviet journal of computer and systems sciences*, 25(6):1–11, 1987.
- [23] Christian Szegedy, Wojciech Zaremba, Ilya Sutskever, Joan Bruna, Dumitru Erhan, Ian Goodfellow, and Rob Fergus. Intriguing properties of neural networks. In *International Conference on Learning Representations*, 2014. URL <http://arxiv.org/abs/1312.6199>.
- [24] Vincent Tjeng, Kai Xiao, and Russ Tedrake. Evaluating robustness of neural networks with mixed integer programming. In *International Conference on Learning Representations*, 2019.
- [25] Irene Waldspurger and Alden Waters. Rank optimality for the burer–monteiro factorization. *SIAM journal on Optimization*, 30(3):2577–2602, 2020.

- [26] Lily Weng, Huan Zhang, Hongge Chen, Zhao Song, Cho-Jui Hsieh, Luca Daniel, Duane Boning, and Inderjit Dhillon. Towards fast computation of certified robustness for ReLU networks. In *International Conference on Machine Learning*, pages 5276–5285, 2018.
- [27] Tsui-Wei Weng, Huan Zhang, Pin-Yu Chen, Jinfeng Yi, Dong Su, Yupeng Gao, Cho-Jui Hsieh, and Luca Daniel. Evaluating the robustness of neural networks: An extreme value theory approach. *arXiv preprint arXiv:1801.10578*, 2018.
- [28] Eric Wong and Zico Kolter. Provable defenses against adversarial examples via the convex outer adversarial polytope. In *International Conference on Machine Learning*, pages 5286–5295, 2018.
- [29] Eric Wong, Leslie Rice, and J Zico Kolter. Fast is better than free: Revisiting adversarial training. In *International Conference on Learning Representations*, 2019.
- [30] Huan Zhang, Tsui-Wei Weng, Pin-Yu Chen, Cho-Jui Hsieh, and Luca Daniel. Efficient neural network robustness certification with general activation functions. *Advances in neural information processing systems*, 31, 2018.
- [31] Richard Y Zhang. On the tightness of semidefinite relaxations for certifying robustness to adversarial examples. In *Advances in Neural Information Processing Systems*, 2020.
- [32] Richard Y Zhang. Improved global guarantees for the nonconvex burer–monteiro factorization via rank overparameterization. *arXiv preprint arXiv:2207.01789*, 2022.
- [33] Richard Y Zhang and Javad Lavaei. Efficient algorithm for large-and-sparse lmi feasibility problems. In *2018 IEEE Conference on Decision and Control (CDC)*, pages 6868–6875. IEEE, 2018.

A Implementation details

In this section, we present the implementation detail of our proposed methods BM, as well as BM-Full, which is an extension of BM with the addition of pre-activation bounds on each hidden neuron. In this section, we focus on the practical formulation of BM and BM-Full for verifying neural networks trained on MNIST dataset.

Valid input set constraints For model train on MNIST dataset, we add an extra constraint $0 \leq u_0 \cdot u_1 \leq 1$ into (BM- r) because MNIST images are normalized to between 0 and 1 during training and testing. Notice that adding an extra inequality constraint $0 \leq u_0 \cdot u_1 \leq 1$ does not alter any theoretical results in this paper as it only add an extra term to s_1 in the slack matrix $S(y, z)$, we will provide more details in the next section.

Simplify constraints in (BM- r) In our practical implementation, we fix u_0 to 1 in (BM- r). The reason is twofold. First, by fixing $u_0 = 1$, most constraints in (BM- r) become linear, and hence reduces the time complexity of our algorithm significantly. Second, the corresponding dual variable, z_0 , can be efficiently estimated via the KKT conditions. We provide more detail on estimating z_0 in the later section.

BM and BM-Full for ℓ_∞ norm To verify robustness of \hat{x} with respect to a ℓ_∞ perturbation, we replace the constraint $\|u_1 - u_0\hat{x}\|^2 + \|V_1\|^2 \leq \rho^2$ in (BM- r) with the elementwise ℓ_2 constraint

$$\text{diag} \left[(u_1 - u_0\hat{x})(u_1 - u_0\hat{x})^T + V_1V_1^T \right] \leq \rho^2.$$

A.1 Practical formulation for BM

We now turn to the practical aspect of implementing our proposed method BM. In particular, to verify neural networks trained on MNIST dataset, we solve (BM- r) in the following form

$$\begin{aligned} \phi_{\text{lb}}(r) &= \min_{u, V} w_\ell^T u_\ell & (8) \\ \text{s.t.} \quad & \|u_1 - \hat{x}\|^2 + \|V_1\|^2 \leq \rho^2, & (y_0) \\ & u_1 \geq 0, \quad u_1 \leq 1 & (y_{0,1}, y_{0,2}) \\ & u_{k+1} \geq 0, \quad u_{k+1} - W_k u_k - b_k \geq 0, & (y_{k,1}, y_{k,2}) \\ & \text{diag} \left[(u_{k+1} - W_k u_k - b_k)u_{k+1}^T + (V_{k+1} - W_k V_k)V_{k+1}^T \right] = 0, & (z_k) \\ & 1 + \sum_{k=1}^{\ell-1} (\|u_k\|^2 + \|V_k\|^2) \leq R^2, & (\mu) \end{aligned}$$

for $k \in \{1, \dots, \ell - 1\}$. Notice that we have substituted $u_0 = 1$, added the valid input set constraints $u_1 \geq 0$ and $u_1 \leq 1$, and assigned their associated dual variable $y_{0,1}$ and $y_{0,2}$. In Definition 8, we summarized how to evaluate the slack matrices $S(y, z)$ and the dual variable z_0 in (SDD) using the primal and dual solution of (8) in order to calculate the bound in Proposition 1.

Definition 8. Let $y = (y_0, \{y_{k,1}, y_{k,2}\}_{k=0}^{\ell-1})$, $z = (\{z_k\}_{k=1}^{\ell-1})$, $u = (u_1, \dots, u_\ell)$ and $V = (V_1, \dots, V_\ell)$ be any *certifiably first-order optimal* point of (8). Each component in the slack matrices $S(y, z)$ and

the dual variable z_0 in (SDD) can be evaluated as

$$\begin{aligned}
s_0 &= -2 \sum_{k=1}^{\ell} s_k^T u_k, \quad z_0 = y_0(\|\hat{x}\|^2 - \rho^2) - 1^T y_{0,2} + \sum_{k=1}^{\ell-1} b_k^T y_{k,2} - \frac{1}{2} s_0, \\
s_1 &= -y_{0,1} + y_{0,2} + W_1^T y_{1,2} - 2\hat{x}y_0, \quad s_{\ell} = w_{\ell} - [Z_{(\ell-1)}b_{(\ell-1)} + y_{(\ell-1),1} + y_{(\ell-1),2}], \\
s_{k+1} &= W_{k+1}^T y_{(k+1),2} - (Z_k b_k + y_{k,1} + y_{k,2}) \quad \text{for } k \in \{1, \dots, \ell-2\}, \\
S_{1,1} &= 2y_0 I, \quad S_{k,(k+1)} = -W_k^T Z_k, \quad S_{(k+1),(k+1)} = 2Z_k \quad \text{for } k \in \{1, \dots, \ell-1\},
\end{aligned}$$

where $Z_k = \text{diag}(z_k)$ for all k .

A.2 Practical formulation for BM-Full

We now describe the practical formulation for **BM-Full**. Let lb_k and ub_k denote the lower bound and the upper bound on neurons x_k in the k -th layer. In order to incorporate the bound constraint $lb_k \leq x_k \leq ub_k$ into **BM**, we rewrite it into a quadratic constraint for which x_k is restricted in a ℓ_2 norm ball centered at $(ub_k + lb_k)/2$ with radius $(ub_k - lb_k)/2$ as in

$$lb_k \leq x_k \leq ub_k \iff \left(x_k - \frac{(ub_k + lb_k)}{2} \right) \odot \left(x_k - \frac{(ub_k + lb_k)}{2} \right) \leq \frac{(ub_k - lb_k)^2}{4}.$$

To verify neural networks trained on MNIST dataset, we solve **BM-Full** in the following form

$$\begin{aligned}
\phi_{\text{lb}}(r) &= \min_{u, V} w_{\ell}^T u_{\ell} & (9) \\
\text{s.t.} \quad & \|u_1 - \hat{x}\|^2 + \|V_1\|^2 \leq \rho^2, & (y_0) \\
& u_1 \geq 0, \quad u_1 \leq 1 & (y_{0,1}, y_{0,2}) \\
& \text{diag} \left[(u_{k+1} - \hat{x}_{k+1})(u_{k+1} - \hat{x}_{k+1})^T + V_{k+1} V_{k+1}^T \right] \leq \rho_{k+1}^2 & (y_k) \\
& u_{k+1} - W_k u_k - b_k \geq 0, & (y_{k,2}) \\
& \text{diag} \left[(u_{k+1} - W_k u_k - b_k) u_{k+1}^T + (V_{k+1} - W_k V_k) V_{k+1}^T \right] = 0, & (z_k) \\
& 1 + \sum_{k=1}^{\ell-1} (\|u_k\|^2 + \|V_k\|^2) \leq R^2, & (\mu)
\end{aligned}$$

for $k \in \{1, \dots, \ell-1\}$, where $\hat{x}_k = (\max\{ub_k, 0\} + \max\{lb_k, 0\})/2$ and $\rho_k = (\max\{ub_k, 0\} - \max\{lb_k, 0\})/2$. Notice that u_k is the postactivation at the k -th layer; hence, $\max\{lb_k, 0\} \leq u_k \leq \max\{ub_k, 0\}$. We also delete the constraint $u_k \geq 0$ because it overlaps with the bound constraint $\max\{lb_k, 0\} \leq u_k$. In Definition 9, we summarized how to evaluate the slack matrices $S(y, z)$ and the dual variable z_0 in (SDD) using the primal and dual solution of (9) in order to calculate the bound in Proposition 1.

Definition 9. Let $y = (y_0, y_{0,1}, y_{0,2}, \{y_k, y_{k,2}\}_{k=1}^{\ell-1})$, $z = (\{z_k\}_{k=1}^{\ell-1})$, $u = (u_1, \dots, u_{\ell})$ and $V = (V_1, \dots, V_{\ell})$ be any *certifiably first-order optimal* point of (9). Each component in the slack matrices

$S(y, z)$ and the dual variable z_0 in (SDD) can be evaluated as

$$\begin{aligned} s_0 &= -2 \sum_{k=1}^{\ell} s_k^T u_k, \quad z_0 = y_0(\|\hat{x}\|^2 - \rho^2) + \sum_{k=1}^{\ell-1} y_k^T (\hat{x}_{(k+1)}^2 - \rho_{(k+1)}^2) - 1^T y_{0,2} + \sum_{k=1}^{\ell-1} b_k^T y_{k,2} - \frac{1}{2} s_0, \\ s_1 &= -y_{0,1} + y_{0,2} + W_1^T y_{1,2} - 2\hat{x}y_0, \quad s_\ell = w_\ell - \left[Z_{(\ell-1)} b_{(\ell-1)} + 2\hat{X}_\ell y_{\ell-1} + y_{(\ell-1),2} \right], \\ s_{k+1} &= W_{k+1}^T y_{(k+1),2} - \left(Z_k b_k + 2\hat{X}_{k+1} y_k + y_{k,2} \right) \quad \text{for } k \in \{1, \dots, \ell-2\}, \\ S_{1,1} &= 2y_0 I, \quad S_{k,(k+1)} = -W_k^T Z_k, \quad S_{(k+1),(k+1)} = 2(Z_k + \hat{X}_k) \quad \text{for } k \in \{1, \dots, \ell-1\}, \end{aligned}$$

where $Z_k = \text{diag}(z_k)$ and $\hat{X} = \text{diag}(\hat{x}_k)$ for all k .

B Derivation of the dual problem

Recall that our primal problem is written (with the corresponding Lagrange multipliers given in parantheses) as the following

$$\begin{aligned} \phi(r) &= \min_{X \in \mathbb{S}^{n+1}} w_\ell^T x_\ell && \text{(SDP-}r\text{)} \\ \text{s.t.} \quad & \text{tr}(X_1) - 2x_1^T \hat{x}_1 + x_0 \|\hat{x}_1\|^2 \leq x_0 \rho^2, \quad x_0 = 1 \quad (y_0, z_0) \end{aligned}$$

subject to the layerwise constraints, for $k \in \{1, \dots, \ell-1\}$

$$\begin{aligned} x_{k+1} &\geq 0, \quad x_{k+1} \geq W_k x_k + b_k x_0, && (y_{k,1}, y_{k,2}) \\ \text{diag}(X_{k+1} - W_k X_{k,(k+1)} - b_k x_{k+1}^T) &= 0, && (z_k) \end{aligned}$$

and over a rank-constrained semidefinite variable

$$X = \left[\begin{array}{c|ccc} x_0 & x_1^T & \cdots & x_\ell^T \\ \hline x_1 & X_{1,1} & \cdots & X_{1,\ell} \\ \vdots & \vdots & \ddots & \vdots \\ x_\ell & X_{1,\ell}^T & \cdots & X_{\ell,\ell} \end{array} \right] \succeq 0, \quad \text{rank}(X) \leq r.$$

This problem can be viewed as a generic instance of the following primal problem

$$\min_{X \succeq 0} \left\{ \langle F, X \rangle : \begin{array}{ll} \mathcal{G}_0(X) \leq 0, & \mathcal{H}_0(X) + 1 = 0, \\ \mathcal{G}_k(X) \leq 0, & \mathcal{H}_k(X) = 0, \end{array} \quad \text{for all } k \in \{1, \dots, \ell-1\} \right\}$$

in which we implicitly define F to satisfy $\langle F, X \rangle = w_\ell^T x_\ell$ and the linear constraint operators are respectively

$$\begin{aligned} \mathcal{G}_0(X) &= \text{tr}(X_1) - 2\hat{x}^T x_1 + (\|\hat{x}\|^2 - \rho^2)x_0, \quad \mathcal{G}_k(X) = \begin{bmatrix} -x_{k+1} \\ W_k x_k + b_k x_0 - x_{k+1} \end{bmatrix}, \\ \mathcal{H}_0(X) &= -x_0, \quad \mathcal{H}_k(X) = \text{diag}(X_{(k+1),(k+1)} - W_k X_{k,(k+1)} - b_k x_{k+1}^T). \end{aligned}$$

The primal problem can be written as the minimax

$$\min_X \max_{y \geq 0, z, S \geq 0} \mathcal{L}(X, y, z, S)$$

with respect to the following Lagrangian

$$\begin{aligned} \mathcal{L}(X, y, z, S) = & \langle F, X \rangle + \langle z_0, \mathcal{H}_0(X) + 1 \rangle + \langle y_0, \mathcal{G}_0(X) \rangle \\ & + \sum_{k=1}^{\ell-1} \left[\left\langle \begin{bmatrix} y_{k,1} \\ y_{k,2} \end{bmatrix}, \mathcal{G}_k(X) \right\rangle + \langle z_k, \mathcal{H}_k(X) \rangle \right] - \langle S, X \rangle \end{aligned}$$

Swapping the minimization and maximization yields the dual problem

$$\max_{y \geq 0, z, S \succeq 0} \min_X \mathcal{L}(X, y, z, S) = \max_{y \geq 0, z} \{z_0 : S(y, z) \succeq 0\}$$

in which the Slack matrix is written

$$S(y, z) = F + \mathcal{G}_0^T(y_0) + \mathcal{H}_0^T(z_0) + \left[\sum_{k=1}^{\ell-1} \mathcal{G}_k^T(y_{k,1}, y_{k,2}) + \sum_{k=1}^{\ell-1} \mathcal{H}_k^T(z_k) \right]$$

and where we use the superscript “ T ” to indicate the adjoint operators.

Finally, we derive an explicit expression for $S(y, z)$. Here, we write out the adjoint operators in terms of the scalar, vector, and matrix components of X :

$$\begin{aligned} \langle X, F \rangle &= \langle x_\ell, w_\ell \rangle \\ \langle X, \mathcal{H}_0^T(z_0) \rangle &= -x_0 z_0 \\ \langle X, \mathcal{G}_0^T(y_0) \rangle &= x_0 y_0 (\|\hat{x}\|^2 - \rho^2) - \langle x_1, 2y_0 \hat{x} \rangle + \langle X_{1,1}, y_0 I \rangle \\ \langle X, \mathcal{G}_k^T(y_{k,1}, y_{k,2}) \rangle &= x_0 y_{k,2}^T b_k + \left\langle \begin{bmatrix} x_k \\ x_{k+1} \end{bmatrix}, \begin{bmatrix} W_k^T y_{k,2} \\ -(y_{k,1} + y_{k,2}) \end{bmatrix} \right\rangle \\ \langle X, \mathcal{H}_k^T(z_k) \rangle &= -\langle x_{k+1}, Z_k b_k \rangle + \left\langle \begin{bmatrix} X_{k,(k+1)} \\ X_{(k+1),(k+1)} \end{bmatrix}, \begin{bmatrix} -W_k^T Z_k \\ Z_k \end{bmatrix} \right\rangle \end{aligned}$$

where $Z_k = \text{diag}(z_k)$. Isolating the vector terms x_1, x_2, \dots, x_ℓ , we see that the following indeed holds

$$\sum_{k=1}^{\ell} \langle x_k, s_k \rangle = \langle x_\ell, w_\ell \rangle - \langle x_1, 2y_0 \hat{x} \rangle + \sum_{k=1}^{\ell-1} \left[\left\langle \begin{bmatrix} x_k \\ x_{k+1} \end{bmatrix}, \begin{bmatrix} W_k^T y_{k,2} \\ -(y_{k,1} + y_{k,2}) \end{bmatrix} \right\rangle - \langle x_{k+1}^T, b_k^T Z_k \rangle \right]$$

with the following definition

$$\begin{aligned} s_1 &= W_1^T y_{1,2} - 2\hat{x} y_0, \quad s_\ell = w_\ell - [Z_{(\ell-1)} b_{(\ell-1)} + y_{(\ell-1),1} + y_{(\ell-1),2}], \\ s_{k+1} &= W_{k+1}^T y_{(k+1),2} - (Z_k b_k + y_{k,1} + y_{k,2}) \quad \text{for } k \in \{1, \dots, \ell-2\}. \end{aligned}$$

It remains to verify that with the following definition

$$\begin{aligned} s_0 &= 2 \left[y_0 (\|\hat{x}\|^2 - \rho^2) + \sum_{k=1}^{\ell-1} b_k^T y_{k,2} - z_0 \right], \\ S_{1,1} &= y_0 I, \quad S_{k,(k+1)} = -W_k^T Z_k, \quad S_{(k+1),(k+1)} = 2Z_k \quad \text{for } k \in \{1, \dots, \ell-1\}, \end{aligned}$$

we indeed have

$$\langle X, S(y, z) \rangle = \frac{1}{2} x_0 s_0 + \sum_{k=1}^{\ell} \frac{1}{2} \langle X_{k,k}, S_{k,k} \rangle + \sum_{k=1}^{\ell} \langle x_k, s_k \rangle + \sum_{j>k} \langle X_{j,k}, S_{j,k} \rangle.$$

C Proof of Constraint Qualification

Lemma 10 (Single neuron). *Let $\bar{\alpha}, \alpha \in \mathbb{R}$ and $\beta, \bar{\beta} \in \mathbb{R}^{r-1}$ satisfy $g_1(\alpha, \beta) \geq 0$ and $g_2(\alpha, \beta) \geq 0$ and $h(\alpha, \beta) = 0$, where*

$$g_1(\alpha, \beta) = \alpha, \quad g_2(\alpha, \beta) = \alpha - \bar{\alpha}, \quad h(\alpha, \beta) = \alpha(\alpha - \bar{\alpha}) + \langle \beta, \beta - \bar{\beta} \rangle.$$

Suppose that $\bar{\alpha} \neq 0$ and $\bar{\beta} \neq 0$. Then, the following holds

$$\begin{aligned} \nabla g_1(\alpha, \beta)y_1 + \nabla g_2(\alpha, \beta)y_2 + \nabla h(\alpha, \beta)z &= 0, \\ g_1(\alpha, \beta) \odot y_1 = g_2(\alpha, \beta) \odot y_2 &= 0, \end{aligned}$$

if and only if $y_1 = y_2 = z = 0$.

Proof. Explicitly computing the Jacobians reveals the desired claim as equivalent to the following

$$\begin{bmatrix} 1 & 1 & 2\alpha - \bar{\alpha} \\ 0 & 0 & 2\beta - \bar{\beta} \\ \alpha & 0 & 0 \\ 0 & \alpha - \bar{\alpha} & 0 \end{bmatrix} \begin{bmatrix} y_1 \\ y_2 \\ z \end{bmatrix} = 0 \quad \iff \quad \begin{bmatrix} y_1 \\ y_2 \\ z \end{bmatrix} = 0. \quad (10)$$

Next, completing the square $\alpha(\alpha - \bar{\alpha}) + \langle \beta, \beta - \bar{\beta} \rangle = \|(\alpha, \beta) - \frac{1}{2}(\bar{\alpha}, \bar{\beta})\|^2 - \|\frac{1}{2}(\bar{\alpha}, \bar{\beta})\|^2$ reveals that

$$h(\alpha, \beta) = 0 \quad \implies \quad \|2(\alpha, \beta) - (\bar{\alpha}, \bar{\beta})\| = \|(\bar{\alpha}, \bar{\beta})\| \quad (11)$$

If additionally $\alpha = \max\{0, \bar{\alpha}\}$, then substituting $\alpha(\alpha - \bar{\alpha}) = 0$ into the above further yields

$$\alpha = \max\{0, \bar{\alpha}\}, \quad h(\alpha, \beta) = 0 \quad \implies \quad \|2\beta - \bar{\beta}\| = \|\bar{\beta}\|. \quad (12)$$

Next, from $|g_1(\alpha, \beta) - g_2(\alpha, \beta)| = |\bar{\alpha}| > 0$, it follows that we cannot jointly have $g_1(\alpha, \beta) = g_2(\alpha, \beta) = 0$ at the same time. We proceed by analyzing the other three cases one at a time:

- If $g_1(\alpha, \beta) = 0$ and $g_2(\alpha, \beta) > 0$, then $y_2 = 0$. Substituting into (10), it follows from $\|2\beta - \bar{\beta}\| = \|\bar{\beta}\| > 0$ via (12) that

$$\begin{bmatrix} 1 & 2\alpha - \bar{\alpha} \\ 0 & 2\beta - \bar{\beta} \end{bmatrix} \begin{bmatrix} y_1 \\ z \end{bmatrix} = 0 \quad \iff \quad \begin{bmatrix} y_1 \\ z \end{bmatrix} = 0.$$

- If $g_1(\alpha, \beta) > 0$ and $g_2(\alpha, \beta) = 0$, then $y_1 = 0$. Substituting into (10), it again follows from $\|2\beta - \bar{\beta}\| = \|\bar{\beta}\| > 0$ via (12) that the following holds

$$\begin{bmatrix} 1 & 2\alpha - \bar{\alpha} \\ 0 & 2\beta - \bar{\beta} \end{bmatrix} \begin{bmatrix} y_2 \\ z \end{bmatrix} = 0 \quad \iff \quad \begin{bmatrix} y_2 \\ z \end{bmatrix} = 0.$$

- Finally, if $g_1(\alpha, \beta) > 0$ and $g_2(\alpha, \beta) > 0$, then both $y_1 = y_2 = 0$. Substituting into (10), it follows from $\|(2\alpha - \bar{\alpha}, 2\beta - \bar{\beta})\| = \|(\bar{\alpha}, \bar{\beta})\| > 0$ via (11) that

$$\begin{bmatrix} 2\alpha - \bar{\alpha} \\ 2\beta - \bar{\beta} \end{bmatrix} z = 0 \quad \iff \quad z = 0.$$

□

Lemma 11 (Single layer). *Let $\bar{u}, u \in \mathbb{R}^n$ and $\bar{V}, V \in \mathbb{R}^{n \times (r-1)}$ satisfy $g_1(u, V) \geq 0$ and $g_2(u, V) \geq 0$ and $h(u, V) = 0$, where*

$$g_1(u, V) = u, \quad g_2(u, V) = u - W\bar{u} - b, \quad h(u, V) = \text{diag}[u(u - W\bar{u} - b)^T + V(V - W\bar{V})^T].$$

Suppose that $\mathbf{e}_i^T(W\bar{u} + b) \neq 0$ and $\mathbf{e}_i^T W\bar{V} \neq 0$ hold for all $i \in \{1, 2, \dots, n\}$. Then, the following holds

$$\begin{aligned} \nabla g_1(u, V)y_1 + \nabla g_2(u, V)y_2 + \nabla h(u, V)z &= 0, \\ g_1(u, V) \odot y_1 &= g_2(u, V) \odot y_2 = 0, \end{aligned}$$

if and only if $y_1 = y_2 = z = 0$.

Proof. Explicitly writing out the Jacobians allows us to restate the desired claim as the following

$$\begin{bmatrix} I & I & \text{diag}(2u - W\bar{u} - b) \\ 0 & 0 & \text{diag}(2v_1 - W\bar{v}_1) \\ \vdots & \vdots & \vdots \\ 0 & 0 & \text{diag}(2v_{r-1} - W\bar{v}_{r-1}) \\ \text{diag}(u) & 0 & 0 \\ 0 & \text{diag}(u - W\bar{u} - b) & 0 \end{bmatrix} \begin{bmatrix} y_1 \\ y_2 \\ z \end{bmatrix} = 0 \iff \begin{bmatrix} y_1 \\ y_2 \\ z \end{bmatrix} = 0.$$

Collecting the diagonal elements, we see that this claim holds true if and only if the following holds true for all $i \in \{1, 2, \dots, n\}$:

$$\begin{bmatrix} 1 & 1 & 2\alpha_i - \bar{\alpha}_i \\ 0 & 0 & 2\beta_i - \bar{\beta}_i \\ \alpha_i & 0 & 0 \\ 0 & \alpha_i - \bar{\alpha}_i & 0 \end{bmatrix} \begin{bmatrix} y_{1,i} \\ y_{2,i} \\ z_i \end{bmatrix} = 0 \iff \begin{bmatrix} y_{1,i} \\ y_{2,i} \\ z_i \end{bmatrix} = 0$$

where $\alpha_i = \mathbf{e}_i^T u$ and $\bar{\alpha}_i = \mathbf{e}_i^T (u - W\bar{u} - b)$ and $\beta_i^T = \mathbf{e}_i^T V$ and $\bar{\beta}_i^T = \mathbf{e}_i^T W\bar{V}$. In turn, given that $\bar{\alpha}_i \neq 0$ and $\bar{\beta}_i \neq 0$ by hypothesis, it follows from Lemma 10 that the above holds true if and only if $y_{1,i} = y_{2,i} = z_i = 0$. \square

Lemma 12 (Multiple layers). *Let $u = (u_1, \dots, u_\ell) \in \mathbb{R}^n$ and $V = (V_1, \dots, V_\ell) \in \mathbb{R}^{n \times (r-1)}$ satisfy $g_{k,1}(u, V) \geq 0$ and $g_{k,2}(u, V) \geq 0$ and $h_k(u, V) = 0$ for all k , where*

$$\begin{aligned} g_{k,1}(u, V) &= u_{k+1}, \quad g_{k,2}(u, V) = u_{k+1} - W_k u_k - b_k, \\ h_k(u, V) &= \text{diag}[u_{k+1}(u_{k+1} - W_k u_k - b_k)^T + V_{k+1}(V_{k+1} - W_k V_k)^T]. \end{aligned}$$

Suppose that $\mathbf{e}_i^T(W_k u_k + b_k) \neq 0$ and $\mathbf{e}_i^T W_k V_k \neq 0$ hold for all $i \in \{1, 2, \dots, n\}$ and all $k \in \{1, 2, \dots, \ell - 1\}$. Then, the following holds

$$\begin{aligned} \sum_{k=1}^{\ell-1} [\nabla g_{k,1}(u, V)y_{k,1} + \nabla g_{k,2}(u, V)y_{k,2} + \nabla h_k(u, V)z_k] &= 0, \\ g_{k,1}(u, V) \odot y_{k,1} &= g_{k,2}(u, V) \odot y_{k,2} = 0 \quad \text{for all } k \in \{1, 2, \dots, \ell - 1\} \end{aligned}$$

if and only if $y_{k,1} = y_{k,2} = z_k = 0$ for all $k \in \{1, 2, \dots, \ell - 1\}$.

Proof. Let us assume $r = 2$ without loss of generality. We observe a block bi-diagonal structure in the Jacobians

$$\frac{\partial g_{k,1}}{\partial u_j} = \begin{cases} I & j = k + 1, \\ 0 & \text{otherwise,} \end{cases} \quad \frac{\partial g_{k,2}}{\partial u_j} = \begin{cases} I & j = k + 1, \\ -W_k & j = k, \\ 0 & \text{otherwise,} \end{cases} \quad \frac{\partial g_{k,1}}{\partial v_j} = \frac{\partial g_{k,2}}{\partial v_j} = 0,$$

and also

$$\frac{\partial h_k}{\partial u_j} = \begin{cases} \text{diag}(2u_k - W_j u_j - b_j) & j = k + 1, \\ -\text{diag}(u_{k+1})W_k & j = j, \\ 0 & \text{otherwise,} \end{cases} \quad \frac{\partial h_k}{\partial v_j} = \begin{cases} \text{diag}(2v_k - W_j v_j) & j = k + 1, \\ -\text{diag}(v_{k+1})W_k & j = k, \\ 0 & \text{otherwise.} \end{cases}$$

This motivates us to rewrite the desired claim as the following

$$\begin{bmatrix} C_1 & & & & \\ D_1 & C_2 & & & \\ & D_2 & \ddots & & \\ & & \ddots & C_{\ell-1} & \\ & & & D_{\ell-1} & \end{bmatrix} \begin{bmatrix} \lambda_1 \\ \lambda_2 \\ \vdots \\ \lambda_{\ell-1} \end{bmatrix} = 0 \quad \iff \quad \begin{bmatrix} \lambda_1 \\ \lambda_2 \\ \vdots \\ \lambda_{\ell-1} \end{bmatrix} = 0. \quad (13)$$

in which $\lambda_k = (y_{k,1}, y_{k,2}, z_k)$ and the blocks are written

$$D_k = \begin{bmatrix} I & I & \text{diag}(2u_{k+1} - W_k u_k - b_k) \\ 0 & 0 & \text{diag}(2v_{k+1} - W_k v_k) \\ \text{diag}(u_{k+1}) & 0 & 0 \\ 0 & \text{diag}(u_{k+1} - W_k u_k - b_k) & 0 \end{bmatrix},$$

$$C_k = - \begin{bmatrix} 0 & W_k^T & W_k^T \text{diag}(u_{k+1}) \\ 0 & 0 & W_k^T \text{diag}(v_{k+1}) \end{bmatrix}.$$

Focusing our attention on the ℓ -th block-row, we apply Lemma 11 and find that $D_{\ell-1}\lambda_{\ell-1} = 0$ implies $\lambda_{\ell-1} = 0$ under our stated hypothesis that $\mathbf{e}_i^T(W_{\ell-1}u_{\ell-1} + b_{\ell-1}) \neq 0$ and $\mathbf{e}_i^T W_{\ell-1}V_{\ell-1} \neq 0$ for all i . Next, substituting $\lambda_{\ell-1} = 0$ into $(\ell - 1)$ -th block-row, we apply Lemma 11 and find that $D_{\ell-2}\lambda_{\ell-2} = -C_{\ell-1}\lambda_{\ell-1} = 0$ implies $\lambda_{\ell-2} = 0$ under our stated hypothesis that $\mathbf{e}_i^T(W_{\ell-2}u_{\ell-2} + b_{\ell-2}) \neq 0$ and $\mathbf{e}_i^T W_{\ell-2}V_{\ell-2} \neq 0$ for all i . Repeating this same argument, we conclude that the left-hand side of (13) does indeed imply the right-hand side under our stated hypotheses, as desired. \square

Theorem 13 (Main). *Let $u_0 \in \mathbb{R}$ and $u = (u_1, \dots, u_\ell) \in \mathbb{R}^n$ and $V = (V_1, \dots, V_\ell) \in \mathbb{R}^{n \times (r-1)}$ satisfy $g_{k,1}(u_0, u, V) \geq 0$ and $g_{k,2}(u_0, u, V) \geq 0$ and $h_k(u_0, u, V) = 0$ for all k , where*

$$\begin{aligned} g_0(u_0, u, V) &= \|u_1 - \hat{x}u_0\|^2 + \|V_1\|^2 - \rho^2, & h_0(u_0, u, V) &= u_0, \\ g_{k,1}(u_0, u, V) &= u_0 u_{k+1}, & g_{k,2}(u_0, u, V) &= u_0 (u_{k+1} - W_k u_k - b_k u_0), \\ h_k(u_0, u, V) &= \text{diag}[u_{k+1}(u_{k+1} - W_k u_k - b_k u_0)^T + V_{k+1}(V_{k+1} - W_k V_k)^T]. \end{aligned}$$

Suppose that $\mathbf{e}_i^T(W_k u_k + b_k) \neq 0$ and $\mathbf{e}_i^T W_k V_k \neq 0$ hold for all $i \in \{1, 2, \dots, n\}$ and all $k \in \{1, 2, \dots, \ell - 1\}$. Then, the following holds

$$\sum_{k=0}^{\ell-1} [\nabla g_{k,1}(u_0, u, V)y_{k,1} + \nabla g_{k,2}(u_0, u, V)y_{k,2} + \nabla h_k(u_0, u, V)z_k] = 0,$$

$$g_{k,1}(u_0, u, V) \odot y_{k,1} = g_{k,2}(u_0, u, V) \odot y_{k,2} = 0 \quad \text{for all } k \in \{0, 1, \dots, \ell - 1\}$$

if and only if $y_{k,1} = y_{k,2} = z_k = 0$ for all $k \in \{0, 1, \dots, \ell - 1\}$.

